J Incl Phenom Macrocycl Chem (2008) 60:253–261
DOI 10.1007/s10847-007-9373-5

ORIGINAL ARTICLE

Effects of cyclodextrins and saccharides on dual fluorescence of *N,N*-dimethyl-4-aminophenylboronic acid in water

Rimiko Ozawa · Takashi Hayashita · Takahiro Matsui · Chiaki Nakayama · Akiyo Yamauchi · Iwao Suzuki

Received: 3 July 2007 / Accepted: 28 August 2007 / Published online: 15 September 2007

Abstract *N,N*-Dimethyl-4-aminophenylboronic acid (DMAPB) showed pH-dependent dual fluorescence at 360 and 462 nm originating from locally excited (LE) and twisted intramolecular charge transfer (TICT) states, respectively, in aqueous solutions. Upon complexation with α-CD, LE fluorescence was markedly increased while TICT fluorescence was decreased. In contrast, both LE and TICT fluorescence were increased when DMAPB was complexed with β-CD. The fluorescence variations enabled us to determine the 1:1 and 1:2 binding constants of the DMAPB/α-CD complex to be 10 and 40 M^{-1}, respectively, and the 1:1 binding constant of the DMAPB/β-CD complex to be 635 M^{-1}. The dual fluorescence of DMAPB alone was found to be a good indicator of saccharide sensing. Under weakly alkaline conditions, saccharides suppressed TICT fluorescence while increasing LE fluorescence. Among the saccharides investigated, D-fructose induced the largest fluorescence change, followed by D-ribose and D-glucose. This order is consistent with the stability of the boronate esters of DMAPB with saccharides. In the presence of β-CD, saccharide selectivity was unchanged, while fluorescence was amplified. These results demonstrate the superiority of the supramolecular DMAPB/β-CD complex to DMAPB alone as a ratiometric fluorescence sensor for saccharides in water.

R. Ozawa · T. Hayashita (✉)
Department of Chemistry, Faculty of Science and Technology, Sophia University, 7-1 Kioicho, Chiyoda-ku, Tokyo 102-8554, Japan
e-mail: ta-hayas@sophia.ac.jp

T. Matsui · C. Nakayama · A. Yamauchi · I. Suzuki (✉)
Graduate School of Pharmaceutical Sciences, Tohoku University, Sendai 980-8578, Japan
e-mail: isuzuki@mail.pharm.tohoku.ac.jp

Keywords Boronic acid · Chemical sensor · Cyclodextrin · Dual fluorescence · Saccharide sensing · Twisted intramolecular charge transfer

Introduction

The formation of the twisted intramolecular charge transfer (TICT) state in certain aromatic compounds has been the source of much intrigue among chemists [1]. Compounds that form the TICT state often show dual fluorescence in which fluorescence appearing at short and long wavelength regions originates from locally excited (LE) and TICT states, respectively. *N,N*-Dimethyl-4-aminobenzonitrile (DMAB), a well-known example of a TICT-state-forming compound, shows dual fluorescence. Figure 1 illustrates the mechanism of dual fluorescence emission by DMAB. Since charge transfer and bond rotation at the photo-excited state are deeply involved in the TICT state formation, many factors including inclusion complex formation affect the dual fluorescence of DMAB. For DMAB, the effect of inclusion complex formation with cyclodextrins (CDs) has been documented [2–6], and the dual fluorescence of DMAB was indeed affected upon complexation with CDs.

Although DMAB has a favorable photophysical property as a chemical sensor, that is, the emission of environmentally sensitive dual fluorescence, the lack of functional groups to participate in typical molecular recognition events has hindered the use of DMAB as a fluorescent chemical sensor. *N,N*-Dimethyl-4-aminophenylboronic acid (DMAPB) is structurally related to DMAB: the boronic acid group of DMAPB is an electron withdrawing group, similar to the carbonitrile group of DMAB. The boronic acid functionality is vital for DMAPB to act as a saccharide receptor. It is well known that

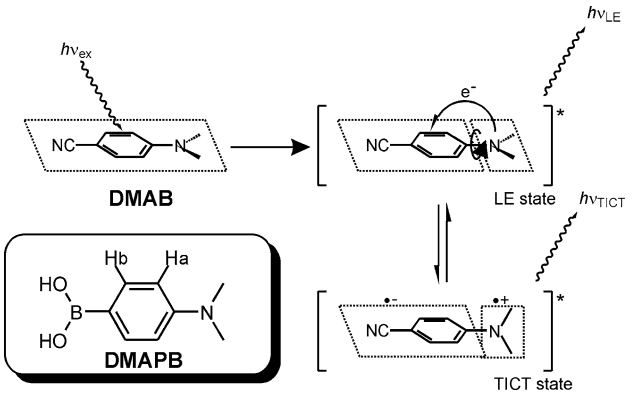

Fig. 1 Schematic representation of the formation of LE (= locally excited) and TICT (= twisted intramolecular charge transfer) states of DMAB. The chemical structure of DMAPB is also shown

arylboronic acids are excellent receptors for saccharides [7–10], and many of them exhibit excellent superior signaling properties, such as color and fluorescence changes upon binding saccharides [11–18]. By combining the potential to form a TICT state with saccharide binding capability, DMAPB is expected to be a good chemical sensor for saccharides. The saccharide binding mechanism of DMAPB is shown in Fig. 2. Since in general, the relationship $K'_S >> K_S$ holds for arylboronic acids [19], the equilibria shown in Fig. 2 indicate that saccharide binding to the boronic acid group generates a negative charge at the boron atom. This negative charge lowers the Lewis acidity of the boron atom drastically, and hence the expected dual fluorescence of DMAPB is affected significantly.

From the viewpoint of chemical sensing, a supramolecular approach may improve the sensing properties of single-molecular-based chemical sensors. We have already reported that the supramolecular approach using CD complexation would enable saccharide sensing by arylboronic acids, enhancing both molecular recognition and fluorescent signaling properties of the dye molecules [20, 21]. That DMAPB has a benzene ring that is recognizable by CDs lead us to another interesting question regarding DMAPB/CD complexes: how does CD complexation affect the fluorescence and saccharide sensing capability of DMAPB?

In this paper, we report the dual fluorescence of DMAPB and its modulation, which is induced by the formation of boronate ester with saccharides, in relation to the inclusion complex formation of DMAPB with α- and β-CDs. The superiority of the supramolecular DMAPB/β-CD complex to DMAPB alone as a ratiometric fluorescence sensor for saccharides is demonstrated.

Experimental

Materials

DMAPB was purchased from Sigma-Aldrich (St. Louis, MO, USA). The DMAPB sample contained considerable amounts of impurities (*N*,*N*-dimethylaniline, as confirmed by ^{1}H NMR). To remove the impurities, DMAPB was dissolved in CH_2Cl_2–THF (1:1) and extracted with 1 M NaOH. Then, the aqueous layer was neutralized with 3 M HCl and extracted with CH_2Cl_2–THF (1:1). The organic layer was washed successively with water and brine. The separated organic layer was dried ($MgSO_4$) and the solvent was removed under reduced pressure. At this stage, signals assigned to impurities were still observed in the ^{1}H NMR spectra. Finally, we attempted recrystallization from aqueous THF to afford a colorless powder. It should be noted that these purification steps must be conducted rapidly, otherwise the solutions containing DMAPB would turn from colorless to purple and finally to black, especially in alkaline solution.

α-CD and β-CD were purchased from Nacalai Tesque (Kyoto, Japan). α-CD was used without further purification, whereas β-CD was recrystallized twice from water. Other chemicals were of the highest grade commercially available.

Apparatus

Fluorescence spectra were recorded with Hitachi F-4000 and Jasco FP-770 spectrofluorometers. Reported fluorescence spectra were uncorrected. UV-visible spectra were recorded with a Shimadzu UV-1650PC spectrophotometer. ^{1}H NMR spectra were recorded on a JEOL ECP 500 (500 MHz for ^{1}H) and ECA 600 (600 MHz for ^{1}H) spectrometers, and the residual HDO peak was used as internal

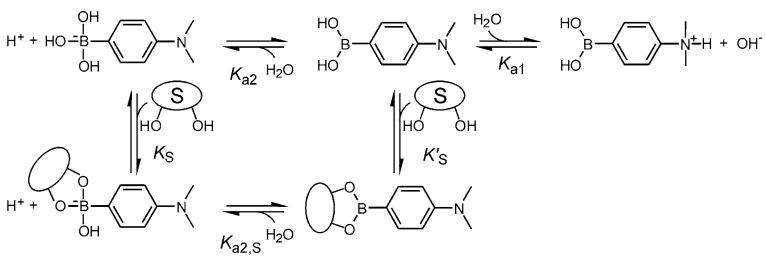

Fig. 2 Acid-base equilibria and boronate ester formation of DMAPB. It is noted that boronate ester formation of the neutral form of boronic acid is negligible ($K'_S \sim 0$)

standard (4.670 ppm from TMS). All measurements were carried out at 25 °C. Owing to the low solubility of DMAPB in pure water, we used 1% (v/v) acetonitrile (MeCN) as co-solvent for photometric and fluorometric measurements, and 10% (v/v) DMSO-d_6 as co-solvent for ^{1}H NMR measurements.

Measurements

UV-visible and fluorescence spectra were measured at 25 °C with appropriate quartz cells. For pH adjustment, 0.01 M phosphates buffer was used, and the ionic strength of the solutions was maintained at 0.1 M with NaCl. For ^{1}H NMR measurements, p*D* was adjusted with D_3PO_4/NaOD (approximately 0.1 M). The excitation wavelength for fluorescence measurements was 273 nm (UV–vis peak maximum) or 251 nm (isosbestic point at various pH values). The former excitation wavelength was used to examine the effects of CDs at constant pH (7.2), whereas the latter was used to obtain the pH profiles.

Determination of acid–base dissociation constants

The acid–base dissociation constants of DMAPB (K_{a1} and K_{a2}) were determined from pH-dependent absorbance changes on the basis of the acid–base equilibria depicted in Fig. 2. Similarly, fluorescence changes were used to determine the acid–base dissociation constants of DMAPB in its excited state (pK^*_{a1} and pK^*_{a2}). The stability constants of boronate esters with saccharides (K_S) were calculated with the following equation:

$$\Delta pK_{a2} = \log\left(K_s[\text{Saccharide}]_0 + 1\right) \quad (1)$$

where ΔpK_{a2} denotes pK_{a2} difference between the absence and presence of saccharides ([Saccharide]$_0$ = 30 mM) [20].

Determination of host–guest binding constants

The binding constants of α- and β-CDs for DMAPB were determined from the fluorescence changes of DMAPB at varying concentrations of α- and β-CDs on the basis of the following equilibria:

$$\alpha\text{-CD} + \text{DMAPB} \overset{K_1}{\rightleftharpoons} \alpha\text{-CD} + \text{DMAPB} \quad (2)$$

$$\alpha\text{-CD} + \alpha\text{-CD:DMAPB} \overset{K_2}{\rightleftharpoons} (\alpha\text{-CD})_2\text{:DMAPB} \quad (3)$$

$$\beta\text{-CD} + \text{DMAPB} \overset{K_1}{\rightleftharpoons} \beta\text{-CD:DMAPB} \quad (4)$$

The fluorescence intensity (F) at any α- or β-CD concentrations is expressed as:

$$F = f_{\text{DMAPB}}[\text{DMAPB}] + f_{\text{CD:DMAPB}}[\text{CD} : \text{DMAPB}] + f_{(\text{CD})_2\text{:DMAPB}}\left[(\text{CD})_2\text{:DMAPB}\right] \quad (5)$$

where f denotes an experimental constant related to the fluorescence intensity of the species specified by subscripts at unit molar concentration. Non-linear regression analyses based on the above equation were performed to obtain K_1 and K_2 [22].

Results and discussion

Dual fluorescence of DMAPB

Figure 3 shows the UV-visible spectra of DMAPB at different pH. A strong absorption band appeared at pH 7.2, and its intensity was decreased under acidic or alkaline conditions. The pK_{a1} and pK_{a2} values of DMAPB were determined to be 4.33 ± 0.01 and 9.49 ± 0.01 from the pH-dependent absorbance changes at 273 nm (inset of Fig. 3). Whereas the pK_{a1} value is approximately the same as the pK_a value of *N*,*N*-dimethylaniline (4.4), the pK_{a2} value is larger than the pK_a value of phenylboronic acid (8.6) by approximately 1 unit, probably due to electron donation by the dimethylamino group. The pK_{a1} and pK_{a2} values demonstrate that DMAPB should be in its neutral form at neutral pH, and that its monocationic and monoanionic forms should be the predominant species at acidic and alkaline pH, respectively. The strong absorption observed at pH 7.2 ($\varepsilon_{272.5} = 1.6 \times 10^4$ M^{-1} cm^{-1}) indicates that the neutral form of DMAPB creates an intramolecular charge transfer (ICT) state in which the boronic acid group is an effective electron acceptor. Under alkaline conditions, the peak was shifted to 244 nm, albeit retaining its intensity to some extent ($\varepsilon_{244} = 1.0 \times 10^4$ M^{-1} cm^{-1}). This suggests that although the anionic boronate group of DMAPB loses its electron accepting ability, the strong electron donating ability of the dimethylamino group retains the ICT nature of DMAPB.

As expected, DMAPB exhibited dual fluorescence typical of a TICT phenomenon [1], with peak maxima at 360 and 462 nm (Fig. 4b) at pH 7. The fluorescence intensities of the two peaks were decreased with decreasing pH, owing to the destabilization of the ICT state caused by the protonation of the amino group of DMAPB. Under alkaline conditions, the intensity of the large red-shifted fluorescence (462 nm band) was decreased more than that of the small red-shifted fluorescence (360 nm band). This

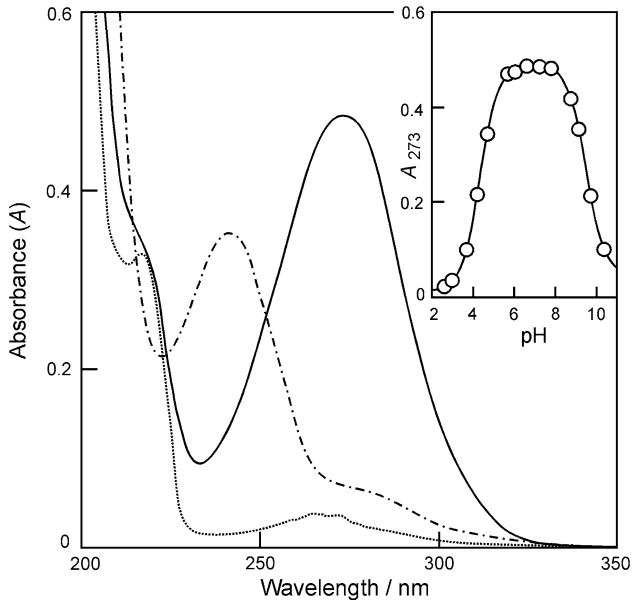

Fig. 3 UV spectra of DMAPB (3.0×10^{-5} M) in aqueous solutions containing 1% (v/v) MeCN at different pH (3.00, dotted line; 7.24, solid line; and 10.38, chain line). Inset shows plots of absorbance at 273 nm as a function of pH. From this pH profile, pK_{a1} and pK_{a2} were determined to be 4.33 and 9.49, respectively

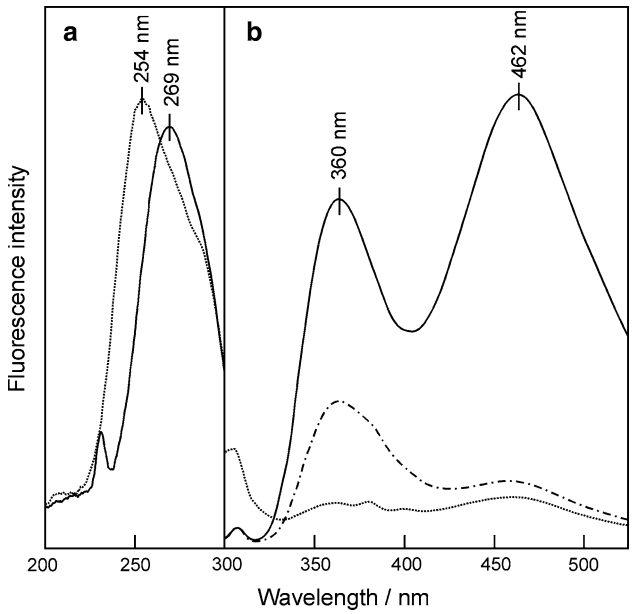

Fig. 4 (a) Fluorescence excitation spectra of DMAPB (3.0×10^{-5} M) in aqueous solutions (pH 7.2, phosphate; $I = 0.07$ M) containing 1% (v/v) MeCN monitored at 462 nm (solid line) and 360 nm (dotted line). (b) Fluorescence spectra of DMAPB (3.0×10^{-5} M; excited at 273 nm) in aqueous solutions containing 1% (v/v) MeCN at different pH (3.07, dotted line; 7.13, solid line; and 10.56, chain line)

pH-dependent fluorescence behavior of DMAPB demonstrates that its dual fluorescence originates in the TICT phenomenon in which the boronic acid group actually acts as an electron acceptor. Thus, the fluorescence with small and large red shifts is attributable to those related to LE and TICT states, respectively.

The fluorescence excitation spectra recorded at LE (360 nm) and TICT (462 nm) fluorescence bands were different, as shown in Fig. 4a. When the excitation spectrum was monitored at the TICT fluorescence band, a peak was observed at 269 nm, which was almost consistent with the UV absorption maximum. In contrast, the excitation spectrum monitored at the LE fluorescence band exhibited a peak maximum at 254 nm. These may result in a high energy barrier for the interconversion between LE and TICT states or different hydrogen bonding capabilities of those two states. Similar phenomena have been reported for *p*-substituted dialkylanilines [4, 5, 23–25].

Effect of CDs

Since the formation of the TICT state accompanies bond rotation at the photo-excited state, a steric factor is expected to influence dual fluorescence emitted at the TICT and LE states. To this end, the inclusion complex formation of DMAB with α- and β-CDs was investigated. The TICT fluorescence of DMAB was reported to show an increase in intensity upon complexation with α-CD [3], whereas both LE and TICT fluorescence showed increases in intensities upon complexation with β-CD [4]. Dimethylaminocarbamoyl CDs, which show dual fluorescence as well, have been studied as fluorescent sensors for organic compounds [26, 27]. Together, these studies imply that the complexation with α- and β-CDs would influence the dual fluorescence of DMAPB.

Figures 5 and 6 show the effects of α- and β-CDs on the fluorescence spectra of DMAPB at pH 7.2. In the presence of α-CD, the LE fluorescence of DMAPB showed prominent increases in intensity with a substantial blue shift (22 nm). In contrast, the TICT fluorescence of DMAPB was decreased upon the addition of α-CD. Although the fluorescence spectra showed an isofluorescence point at 430 nm, binding analysis assuming only the 1:1 complexation process did not reproduce the experimental fluorescence changes; rather, a sequential binding model in which a 1:1 complex was transformed into a 2:1 (α-CD:DMAPB) complex (Eqs. 2 and 3) excellently fitted the experimental data. Binding analysis (inset of Fig. 5) gave binding constants of 10 ± 6 and 40 ± 20 M^{-1} for the first (K_1) and second (K_2) binding processes, respectively. The small K_1 value indicates that the DMAPB molecule is larger than the α-CD cavity. Once the 1:1 complex is formed, the second α-CD molecule easily binds to the 1:1 complex, as evidenced by the large K_2 value. It is known that association dimers of CDs tend to form a "face-to-face" conformation in which the wider mouths of the CDs

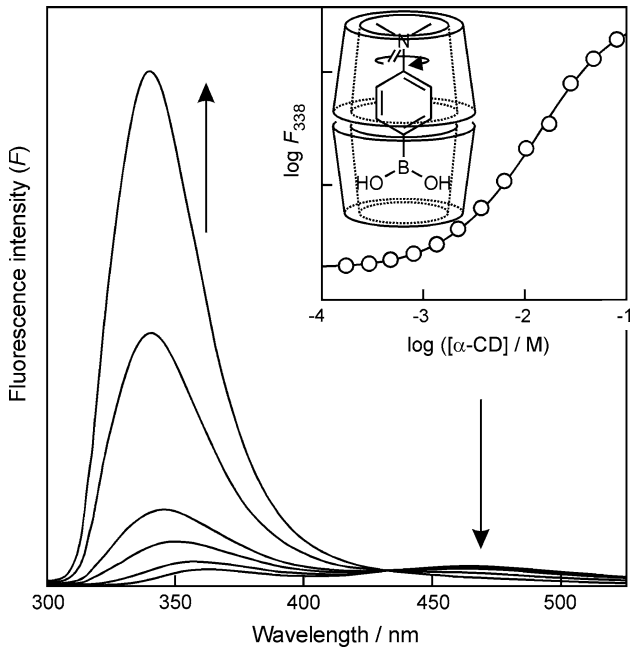

Fig. 5 Fluorescence spectra of DMAPB (3.0×10^{-5} M; excited at 273 nm) in aqueous solutions (pH 7.2) containing 1% (v/v) MeCN and α-CD at various concentrations (0, 1.3, 6.2, 10, 29, and 80 mM). Inset shows plots of fluorescence intensity at 338 nm as a function of α-CD concentration. The solid line is the best-fit binding curve with $K_1 = 10$ and $K_2 = 40$ M^{-1}. The proposed structure of the 2:1 complex (α-CD:DMAPB) is also included

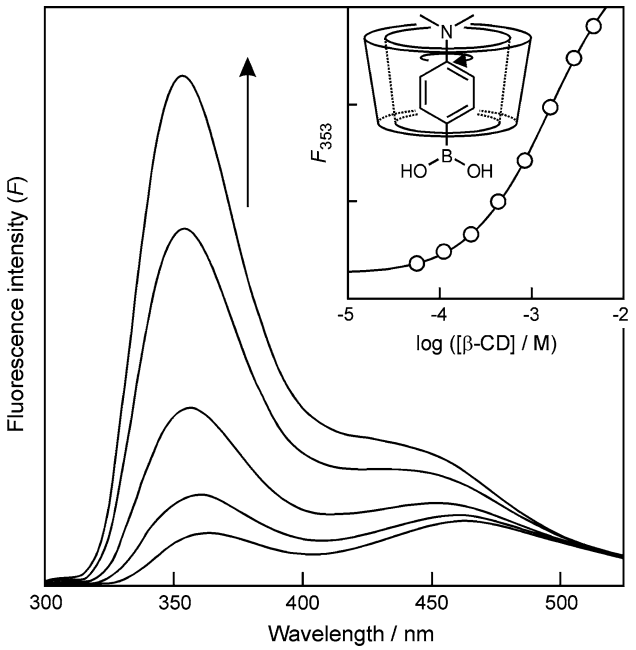

Fig. 6 Fluorescence spectra of DMAPB (3.0×10^{-5} M; excited at 273 nm) in aqueous solutions (pH 7.2) containing 1% (v/v) MeCN and β-CD (0, 0.11, 0.43, 1.6, and 4.7 mM) at various concentrations. Inset shows plots of fluorescence intensity at 353 nm as a function of β-CD concentration. The solid line is the best-fit binding curve with $K_1 = 635$ M^{-1}. The proposed structure of the 1:1 complex (β-CD:DMAPB) is also included

face each other [28, 29]. Taking this trend into consideration, we propose the structure of the 2:1 complex of α-CD with DMAPB, as illustrated in Fig. 5.

In contrast to the α-CD/DMAPB system, the β-CD/DMAPB system formed a simple 1:1 complex as judged from the excellent fit of the theoretical binding curve to the experimentally measured fluorescence (inset of Fig. 6). Binding analysis gave a K_1 value of 635 ± 13 M^{-1} for the β-CD/DMAPB complex, which is larger than the value for the α-CD/DMAPB complex and reflects the large cavity of β-CD, well accommodating a DMAPB molecule.

The large increase in the LE fluorescence observed in the presence of either α- or β-CD indicates that the environment surrounding DMAPB became hydrophobic. The larger enhancement achieved at higher concentrations of α-CD suggests that the DMAPB molecule complexed with α-CD existed in a more hydrophobic environment than that complexed with β-CD. This supports the formation of the $(\alpha\text{-CD})_2$/DMAPB complex, because the "barrel"-like structure of the α-CD association dimer effectively insulated the bound DMAPB molecule from water molecules. The large blue shift of the LE fluorescence (>22 nm) induced by α-CD may have resulted from the full accommodation of DMAPB by two molecules of α-CD. On the other hand, the modest (7 nm) blue shift of the LE fluorescence of DMAPB in the presence of β-CD suggests that DMAPB accommodated in the β-CD cavity is not protected completely from water molecules.

The cavity size difference straightforwardly reflects the TICT fluorescence. Since the TICT state formation of DMAPB requires rotation about the C–N bond, the tight inclusion of DMAPB in the α-CD cavities would hinder this bond rotation, making it difficult for the DMAPB molecule accommodated in α-CD to attain its TICT state, and thereby suppressing TICT fluorescence. In contrast, the large cavity of β-CD would allow rotation about the C–N bond of DMAPB by which the TICT state can be formed, and the TICT state is stabilized by the modest hydrophobicity of the β-CD cavity.

The ground state structure of the DMAPB/β-CD complex was estimated from 2D-ROESY measurements. Figure 7 shows a partial 2D-ROESY spectrum of a mixture of DMAPB (1.5 mM) and β-CD (14 mM) in DMSO-d_6–D_2O (1:9, buffered with phosphate, p*D* 7.6). Weak but distinct ROE correlations of Ha/H′3, Hb/H′3, and Hb/H′5 were observed. The ROE correlation of Hb/H′5 was stronger than that of Hb/H′3. Both H′3 and H′5 oriented towards the interior of the β-CD cavity are positioned near the secondary hydroxyl (wide mouth) and primary hydroxyl (narrow mouth) sides, respectively. Thus, the ROESY spectrum indicates that the major conformation of the DMAPB/β-CD complex is as depicted in the inset of

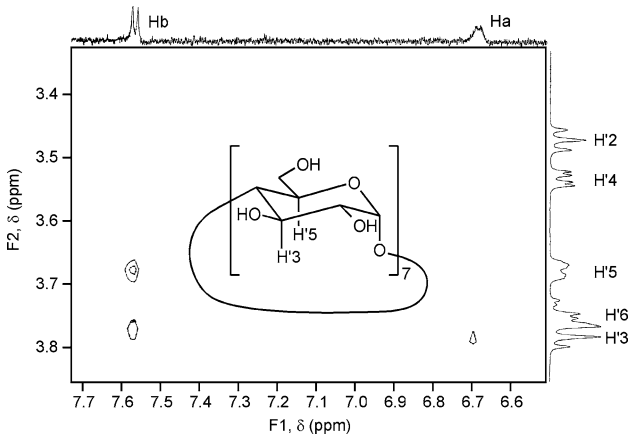

Fig. 7 2D-ROESY spectrum of a β-CD (14 mM)/DMAPB (1.5 mM) system in DMSO-d_6–D_2O (p*D* 7.6). Mixing time was 0.5 s

Fig. 6. The 1D slice of the 2D-ROESY spectrum shows that the Ha doublet was broadened substantially compared with the Hb doublet. The singlet at 2.83 ppm, which was assigned to dimethylamino protons, was also broadened (data not shown). We speculate that the observed signal broadening may be due to the wideness of the secondary hydroxyl side of the β-CD cavity; when the dimethylamino group side of DMAPB is positioned at the secondary hydroxyl side, the molecular motion of that part is partially restricted. In addition, the wideness of the secondary hydroxyl side of the β-CD cavity may provide access to solvent molecules, enabling them to interact with the bound DMAPB. Those two factors may be responsible for the conformational fluctuation of bound DMAPB, broadening the Ha doublet and the singlet of dimethylamino protons.

Effect of saccharides

Since DMAPB has a boronic acid functionality, it is expected to form boronate esters with saccharides in water. From the viewpoint of saccharide sensing, many fluorescent boronic acid derivatives have been synthesized and investigated in terms of fluorescence signaling and saccharide binding properties [11–18, 20, 21]. The large pK_{a2} value of DMAPB (9.49) indicates that it is not a suitable receptor for saccharides in neutral aqueous solutions. However, it is interesting to investigate the fluorescence signaling property of DMAPB under weakly alkaline conditions because it exhibits dual fluorescence in such solutions.

Figure 8a shows the pH-dependent fluorescence profiles of DMAPB with and without D-(–)-fructose (D-fru; 30 mM). It is evident that both LE and TICT fluorescence intensities of DMAPB alone were weak when pH was below 5. The intensities of the LE and TICT fluorescence were also decreased when pH was above 9. The degree of suppression of the TICT fluorescence was more pronounced than that of the LE fluorescence. Under pH conditions above pK_{a2}, DMAPB should exist in its anionic form in which the ICT nature is suppressed, and therefore the LE fluorescence is observed as the predominant emission.

The above-mentioned fluorescence profiles were used to determine the acid–base dissociation constants of DMAPB at the photo-excited state, namely, pK^*_{a1} and pK^*_{a2} values of 4.12 ± 0.01 and 9.71 ± 0.01, respectively. The fact that these values do not deviate markedly from the acid–base dissociation constants of DMAPB at the ground state (pK_{a1} = 4.33 and pK_{a2} = 9.49) indicates that the acid–base dissociation equilibrium is hardly affected by the photo-excitation [30].

When D-fru (30 mM) was added, the TICT fluorescence was decreased when pH was above 6. The suppression of the TICT fluorescence can be explained by the fact that saccharide binding to the boronic acid group facilitates the coordination of the hydroxyl anion to the boron atom. In the pH-dependent fluorescence profile of DMAPB, any effects of saccharides, thus, appear as a shift in pK_{a2} and pK^*_{a2} values. As seen in the pH-dependent TICT fluorescence

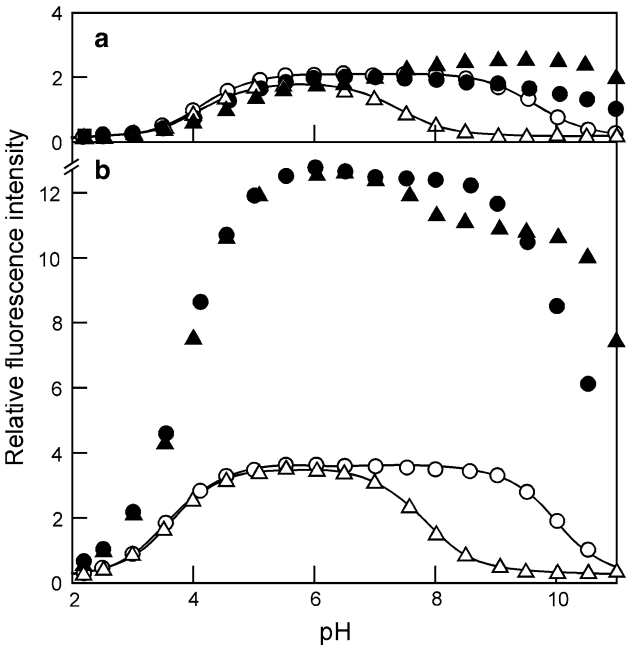

Fig. 8 Plots of LE (360 nm, closed symbols) and TICT (462 nm, open symbols) fluorescence intensities of DMAPB alone (3.0×10^{-5} M; a) or in the presence of β-CD (5 mM; b) as a function of pH. Circles and triangles indicate data obtained without and with D-fru (30 mM), respectively. Lines are best-fit curves of the TICT fluorescence data calculated by non-linear regression analyses

profile, the presence of 30 mM D-fru shifts the pK_{a2}^{*} value of DMAPB from 9.71 to 7.40, which corresponds to the K_S value of 6.8×10^3 M^{-1}. The K_S value of DMAPB with D-fru (5.5×10^3 M^{-1}) was also obtained from the pK_{a2} shift. The fairly good agreement between the K_S values obtained from fluorescence and absorbance data indicates that saccharide binding of DMAPB was hardly affected by the photo-excitation. The obtained K_S value is comparable to or even larger than that of phenylboronic acid (5.6×10^3 M^{-1}) [31], demonstrating that DMAPB is an excellent host for saccharides in weakly alkaline solutions.

The pH-dependent LE fluorescence profile of DMAPB in the presence of D-fru shows slightly increased LE fluorescence intensities at mildly alkaline pH. Above pH = pK_{a2}^{*}, the major fluorescent species should be changed from the neutral to the anionic form of DMAPB. Thus, the increased fluorescence intensity at 360 nm at mildly alkaline pH (8–10) suggests that the fluorescence of the anionic form of DMAPB is enhanced by the complexation with D-fru. On the other hand, the decrease in fluorescence intensity above pH 10 in the presence of D-fru may be due to photo-bleaching. We noticed that DMAPB was relatively unstable under alkaline conditions, as described in the Experimental Section.

Saccharide selectivity was checked by using D-(+)-glucose (D-glc) and D-(+)-ribose (D-rib) together with D-fru. Many boronic acid derivatives show saccharide selectivity that follows the order D-fru > D-rib > D-glc, similar to the order of stability of boronate esters of DMAPB with saccharides. The apparent pK_a and pK_a^{*} values of DMAPB are summarized in Table 1. Similar to other boronic acid derivatives, DMAPB showed saccharide selectivity of D-fru ($K_S = 5.5 \times 10^3$ M^{-1}) > D-rib ($K_S = 9.7 \times 10^2$ M^{-1}) > D-glc ($K_S = 9.9 \times 10^1$ M^{-1}). It is noted that the addition of saccharides hardly affected the pK_{a1} and pK_{a1}^{*} values of DMAPB as expected, because DMAPB loses its saccharide binding ability at low pH.

Saccharide sensing with DMAPB and DMAPB/β-CD complex system

It has been reported that a fluorescent boronic acid gained saccharide sensing ability after complexation with β-CD [20], and the resulting boronic acid/β-CD complex is regarded as a supramolecular fluorescent sensor for saccharides. For DMAPB, it is expected that the fluorescence responses for saccharides would be modified on complexation with CDs. α-CD was not investigated any further because a high concentration of α-CD is required for fluorescence variations. Moreover, the fact that α-CD diminishes the TICT fluorescence of DMAPB while increasing notably its LE fluorescence is disadvantageous for the ratiometric sensing of saccharides. Thus, we focused on the effect of β-CD on the fluorescence responses of DMAPB for saccharides.

Figure 8b shows the pH-dependent fluorescence profiles of DMAPB in the presence of 5 mM β-CD. In the presence of β-CD, the apparent pK_{a1}^{*} and pK_{a2}^{*} values were determined to be 3.58 ± 0.01 and 10.05 ± 0.01, respectively, from the TICT fluorescence changes. These values are smaller and larger than the corresponding pK_{a1}^{*} (4.12) and pK_{a2}^{*} (9.71) values, respectively, indicating that β-CD prefers the neutral form to the cationic and anionic forms of DMAPB for the formation of an inclusion complex. This is reasonable because in general, β-CD tends to form a stable complex with a neutral guest. A similar result was obtained from the absorbance changes.

The addition of D-fru to the DMAPB/β-CD complex solution affected the pK_{a2}^{*} value of DMAPB but not the

Table 1 Acid–base Dissociation Constants (pK_a) of DMAPB in Water Containing 1% (v/v) MeCN[a]

Additive	pK_{a1}[b]	pK_{a2}[b]	pK_{a1}^{*}[c]	pK_{a2}^{*}[c]
None	4.33 ± 0.01	9.49 ± 0.01	4.12 ± 0.01	9.71 ± 0.01
D-fru (30 mM)	4.28 ± 0.03	7.27 ± 0.04 (5500)	4.13 ± 0.01	7.40 ± 0.01 (6770)
D-rib (30 mM)	4.44 ± 0.06	8.01 ± 0.03 (973)	4.16 ± 0.01	8.18 ± 0.01 (1090)
D-glc (30 mM)	4.32 ± 0.01	8.89 ± 0.03 (99.4)	4.17 ± 0.01	9.08 ± 0.01 (107)
β-CD (5 mM)	3.78 ± 0.04	9.90 ± 0.26	3.58 ± 0.02	10.05 ± 0.03
β-CD (5 mM) + D-fru (30 mM)	3.66 ± 0.20	7.78 ± 0.04[d] (4360)[d]	3.62 ± 0.02	7.82 ± 0.03[d] (5630)[d]
β-CD(5 mM) + D-rib (30 mM)	3.83 ± 0.05	8.27 ± 0.03[d] (1390)[d]	3.61 ± 0.02	8.57 ± 0.03[d] (973)[d]
β-CD (5 mM) + D-glc (30 mM)	3.94 ± 0.33	9.37 ± 0.09[d] (79.6)[d]	3.57 ± 0.01	9.52 ± 0.01[d] (79.6)[d]

[a] pK_a and pK_a^{*} values obtained in the presence of any additives are conditional (apparent) values. Values in parentheses are corresponding K_S values calculated with Eq. 1

[b] Determined from absorbance changes at 273 nm

[c] Determined from TICT fluorescence intensity changes around 460 nm (varied by additives)

[d] Conditional values in the presence of 5 mM β-CD

pK^*_{a1} value. The addition of 30 mM D-fru shifted the pK^*_{a2} value from 10.05 to 7.82. However, the extent of the shift (ΔpK^*_{a2}, 2.23) is comparable to that in the absence of β-CD (2.31). This suggests that the boronate ester of DMAPB with D-fru may exhibit affinity towards β-CD in a manner similar to the simple anionic form of DMAPB.

The formation of boronate esters of DMAPB with saccharides in the presence of β-CD decreased the LE fluorescence. This contrasts the case of DMAPB alone for which a slight but obvious increase in LE fluorescence was observed in association with the boronate ester formation (Fig. 8a). Since the boronate ester form of DMAPB bears a negative charge, it is not a suitable guest for β-CD. As a consequence, when D-fru (or another saccharide) is present, the effective concentration of the neutral form of DMAPB to be incorporated into the β-CD cavity is decreased. Thus, in the presence of β-CD, although the boronate ester of DMAPB emits stronger fluorescence than DMAPB alone, the weaker binding of the boronate ester form to β-CD results in the decreased LE fluorescence.

However, the DMAPB/β-CD system has an advantage over DMAPB alone as a fluorescent saccharide sensor, because the fluorescence intensity of DMAPB is enhanced by complexation with β-CD. Moreover, when the ratios of LE to TICT fluorescence intensities of the DMAPB/β-CD system were plotted against pH, the effect of β-CD appeared. As shown in Fig. 9, the LE/TICT fluorescence intensity ratio in the presence of β-CD exceeded 30 at pH 10 when 30 mM D-fru was added. Under the same condition, although DMAPB alone also showed the LE/TICT fluorescence intensity ratio (data not shown), the ratio was approximately 13, which was less than half of that in the presence of β-CD. This is due to the enhancement of the LE fluorescence of DMAPB caused by the formation of an inclusion complex with β-CD. With regard to saccharide selectivity, the largest increase in fluorescence ratio at pH 10 was achieved by D-fru, followed by D-rib and D-glc. This order is consistent with the stability of the boronate esters of DMAPB with saccharides, and hence β-CD does not affect the saccharide selectivity of DMAPB. Consequently, efficient ratiometric sensing for saccharides is achieved with the supramolecular DMAPB/β-CD complex under weakly alkaline conditions.

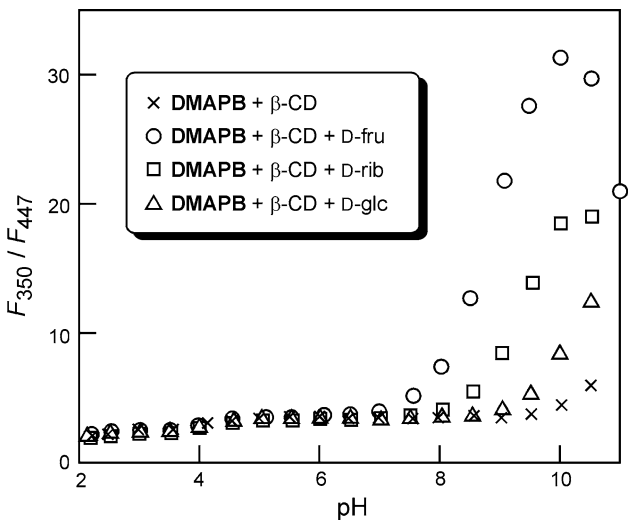

Fig. 9 Plots of LE/TICT fluorescence intensity ratio of the DMAPB (0.03 mM)–β-CD (5 mM) system, alone or in the presence of saccharides (30 mM)

Conclusion

We showed that DMAPB, a structurally related compound of DMAB, exhibited dual fluorescence in aqueous solution. pH titration experiments together with studies of complexation with CDs and saccharides revealed that the dual fluorescence originated in the formation of the TICT state. With regard to the fluorescence sensing, DMAPB alone and its supramolecular system with β-CD were found to act as ratiometric fluorescent sensors for saccharides. Although they function in the pH range of 8 to 10 but do not work under neutral conditions, our results are expected to contribute to the design of fluorescent sensors for saccharides and other analytes, which exhibit dual fluorescence due to the TICT phenomenon.

Acknowledgements This work was supported by Grants-in-Aid for Scientific Research from the Japan Society of Promotion of Science (18350043 and 19550130) and the Toray Scientific Foundation.

References

1. Rettig, W.: Charge separation in excited states of decoupled systems: TICT compounds and implications regarding the development of new laser dyes and the primary processes of vision and photosynthesis. Angew. Chem. Int. Ed. Engl. **25**, 971–988 (1986)
2. Cox, G. S., Hauptman, P. J., Turro, N. J.: Dialkylaminobenzonitriles as fluorescence polarity probes for aqueous solutions of cyclodextrins. Photochem. Photobiol. **39**, 597–601 (1984)
3. Nag, A., Bhattacharyya, K.: Twisted intramolecular charge transfer emission of dimethylaminobenzonitrile in α-cyclodextrin cavities. Chem. Phys. Lett. **151**, 474–476 (1988)
4. Nag, A., Dutta, V., Chattopadhyay, N., Bhattacharyya, K.: Effect of cyclodextrin cavity size on the twisted intramolecular charge transfer emission: dimethylaminobenzonitrile in β-cyclodextrin. Chem. Phys. Lett. **157**, 83–86 (1989)
5. Nag, A., Bhattacharyya, K.: Dual luminescence of dimethylaminobenzonitrile in γ-cyclodextrin—Environmental effects on twisted intramolecular charge-transfer phenomenon. J. Chem. Soc., Faraday Trans. **86**, 53–54 (1990)
6. Banu, H. S., Pitchumani, K., Srinvasan, C.: Dual emission from 4-dimethylaminobenzonitrile in cyclodextrin derivatives. J. Photochem. Photobiol. A: Chemistry **131**, 101–110 (2000)
7. Weith, H. L., Wiebers, J. L., Gilham, P. T.: Synthesis of cellulose derivatives containing the dihydroxyboryl group and a study of

their capacity to form specific complexes with sugars and nucleic acid components. Biochemistry **9**, 4396–4401 (1970)
8. Soundararajan, S., Badawi, M., Kohlrust, C. M., Hageman, J. H.: Boronic acids for affinity chromatography: spectral methods for determinations of ionization and diol-binding constants. Anal. Biochem. **178**, 125–134 (1989)
9. Norrild, J. C., Eggert, H.: Evidence for mono- and bisdentate boronate complexes of glucose in the furanose form. Application of 1JC-C coupling constants as a structural probe. J. Am. Chem. Soc. **117**, 1479–1484 (1995)
10. Nicholls, M. P., Paul, K. C.: Structures of carbohydorate-boronic acid complexes determined by NMR and molecular modeling in aqueous alkaline media. Org. Biomol. Chem. **2**, 1434–1441 (2002)
11. James, T. D., Linnane, P., Shinkai, S.: Fluorescent saccharides receptors: a sweet solution to the design, assembly and evaluation of boronic acid derived PET sensors. Chem. Commun. **11**(3), 281–288 (1996)
12. Lützen, A.: Carbohydrates, Recognition of. In: Atwood J. L., Steed J. N. (eds), Encyclopedia of Supramolecular Chemistry, pp 169–177. Marcel Dekker, New York (2004)
13. Geddes, C. D., Lakowicz, J. R. (eds.): Glucose Sensing (Topics in Fluorescence Spectroscopy, vol. 11), Springer, New York (2006)
14. Sun, X. -Y., Liu, B.: The fluorescence sensor for saccharide based on internal conversion. Luminescence **20**, 331–333 (2005)
15. Zhang, Y., Gao, Z., Hardcastle, K., Wang, B.: Water-soluble fluorescent boronic acid compounds for saccharide sensing substituents effect on their fluorescence properties. Chem. Eur. J. **12**, 1377–1384 (2006)
16. Dowlut, M., Hall, D. G.: An improved class of sugar-binding boronic acids, soluble and capable of complexing glycosides in neutral water. J. Am. Chem. Soc. **128**, 4226–4227 (2006)
17. Gao, Z., Zhang, X., Wang, B.: A highly fluorescent water-soluble boronic acid reporter for saccharide sensing that shows ratiometric UV changes and significant fluorescence changes. Tetrahedron **61**, 9111–9117 (2005)
18. Tan, W., Zhang, D., Wang, Z., Li, C., Zhu, D.: 4-(*N,N*-Dimethylamine)benzonitrile (DMABN) derivatives with boronic acid and boronate groups: new fluorescent sensors for saccharides and fluoride ion. J. Mater. Chem. **17**, 1964–1968 (2007)
19. Lorand, J. P., Edwards, J. O.: Polyol complexes and structure of the benzeneboronate ion. J. Org. Chem. **24**, 769–774 (1959)
20. Tong, A. -J., Yamauchi, A., Hayashita, T., Zhang, Z. -Y., Smith, B. D., Teramae, N.: Boronic acid fluorophore/β-cyclodextrin complex sensors for selective sugar recognition in water. Anal. Chem. **73**, 1530–1536 (2001)
21. Yamauchi, A., Sakashita, Y., Hirose, K., Hayashita, T., Suzuki, I.: Pseudorotaxane-type fluorescent receptor exhibiting unique response to saccharides. Chem. Commun. **41**, 4312–4314 (2006)
22. Suzuki, I., Yamauchi, A.: Pseudo[3]rotaxane type complexation between α- and β-cyclodextrins and *N,N′*-diheptyl-4,4'-bipyridinium. J. Inclusion. Phenom., **54** 193–200 (2006)
23. Rettig, W., Wermuth, G., Lippert, E.: Photophysical primary processes in solutions of *p*-substituted dialkylanilines. Ber. Bunsenges. Phys. Chem. **83**, 692–697 (1979)
24. Al-Hassan, K. A., Rettig, W.: Free-volume sensing fluorescent-probes. Chem. Phys. Lett. **126**, 273–279 (1986)
25. Hrnjez, B. J., Yazdi, P. T., Fox, M. A., Johnston, K. P.: TICT fluorescence emission dependence on excitation wavelength for ethyl *p*-(dimethylamino)benzoate in supercritical trifluoromethane. J. Am. Chem. Soc. **111**, 1915–1916 (1989)
26. Hamasaki, K., Ikeda, H., Nakamura, A., Ueno, A., Toda, F., Suzuki, I., Osa, T.: Fluorescent sensors of molecular recognition: modified cyclodextrins capable of exhibiting guest-responsive twisted intramolecular charge-transfer fluorescence. J. Am. Chem. Soc. **115**, 5035–5040 (1993)
27. Hamasaki, K., Ueno, A., Toda, F.: A fluorescent α-cyclodextrin as a sensor for detecting aliphatic-alcohols by dual fluorescence arising from normal planar and twisted intramolecular charge-transfer excited-states. J. Chem. Soc., Chem. Commun. **3**, 331–333 (1993)
28. Hamai, S.: Pyrene excimer formation in γ-cyclodextrin solutions: Association of 1–1 pyrene-γ-cyclodextrin inclusion compounds. J. Phys. Chem. **93**, 6527–6529 (1989)
29. Miyake, K., Yasuda, S., Harada, A., Sumaoka, J., Komiyama, M., Shigekawa, H.: Formation process of cyclodextrin necklace—analysis of hydrogen bonding on a molecular level. J. Am. Chem. Soc. **125**, 5080–5085 (2003)
30. Ireland, J. F., Wyatt, P. A. H.: Acid–base properties of electronically excited states of organic molecules. Adv. Phys. Org. Chem. **12**, 131–221 (1976)
31. Lorand, J. P., Edwards, J. O.: Polyol complexes and structure of the benzeneboronate ion. J. Org. Chem. **24**, 769–774 (1959)